Rôle of Contrast Media Viscosity in Altering Vessel Wall Shear Stress and Relation to the Risk of Contrast Extravasations

Sophia Sakellariou[1] MBChB, **Wenguang Li**[2] PhD, **Manosh C Paul**[2*] PhD, **Giles Roditi**[1] FRCR, FRCP

[1]Department of Diagnostic Imaging, Glasgow Royal Infirmary, Glasgow G31 2ER, UK

[2]School of Engineering, University of Glasgow, Glasgow G12 8QQ, UK

*Correspondence: Manosh.Paul@glasgow.ac.uk, Tel: +44 (0)141 330 8466; s.sakellariou@nhs.net

Abstract

Iodinated contrast media (CM) are the most commonly used injectables in Radiology today. A range of different media are commercially available, combining various physical and chemical characteristics (ionic state, osmolality, viscosity) and thus exhibiting distinct in vivo behaviour and safety profiles. In this paper, numerical simulations of blood flow with contrast media were conducted to investigate the effects of contrast viscosity on generated vessel wall shear stress and vessel wall pressure to elucidate any possible relation to extravasations. Five different types of contrast for Iodine fluxes ranging at 1.5 gI/s–2.2 gI/s were modelled through 18G and 20G cannulae placed in an ideal vein at two different orientation angles. Results demonstrate that the least viscous contrast media generate the least maximum wall shear stress as well as the lowest total pressure for the same flow rate. This supports the empirical clinical observations and hypothesis that more viscous contrast media are responsible for a higher percentage of contrast extravasations. In addition, results support the clinical hypothesis that a catheter tip directed obliquely to the vein wall always produces the highest maximum wall shear stress and total pressure due to impingement of the contrast jet on the vessel wall.

Keywords: Contrast media, blood flow, numerical modelling, wall shear stress, extravasation

1. Introduction

The roles of ionicity and high versus lower osmolality have been investigated in various studies [1] with the result that non-ionic low osmolar contrast media (LOCM) and iso-osmolar contrast media are now clinically favoured. Viscosity of contrast media has only been studied in relation to the issue of contrast-induced nephrotoxicity and has been found to be a significant parameter through its effects on flow within small intrarenal vessels [2, 3]. Nephrotoxicity refers to the disease of the kidneys, caused from a poisonous effect of toxic chemicals and medications. Generally, contrast media are more viscous and have greater osmolality than blood, plasma, or cerebrospinal fluid. Viscosity and osmolality play a part in the development of contrast reactions, such as anaphylactoid reactions and nephrotoxicity as well as contributing to local tissue toxicity when extravasation occurs [1].

Extravasation of CM into the local soft tissues around the vein at the injection site can occur during hand or power injection in 0.1%–0.9% of cases but this is more common with pump injections which can generate high pressures. The elderly, infants, children, patients with altered consciousness and those with underlying vascular disease are more prone to extravasation [4, 5]. Small volume extravasations of CM result in minor (pain, swelling) or no effect to the patient, but larger extravasations may result in serious effects including skin ulceration, soft-tissue necrosis, and compartment syndrome [6] with subsequent requirements for tissue debridement and/or surgical intervention. Even minor contrast extravasations are, however, important from the patient perspective, as there is a perceived impression that 'something has gone wrong'.

With CT angiography (CTA) techniques the attenuation in the vessel of interest is predicated upon the dynamics of the CM injection – the flow rate, iodine concentration of the CM and the use of saline chasing flush all influence the achieved contrast density in the target vessel for any given patient. Patient factors also influence this (particularly cardiac output) though these can generally not be influenced for the purposes of improving scan quality. Hence the main variable that can be modified is the iodine flux (gI/sec) which is the product of the CM concentration and injection rate. High iodine flux rates produce higher vascular opacification, which in general is desirable, especially in the recently rapidly burgeoning CTA field of cardiac/coronary imaging. However, the high CM flow rates required to produce high iodine flux are recognised to increase the risk of extravasation. As viscosity describes the 'thickness' of CM or its resistance to flow, it is hypothesised that lower viscosity contrast media should lower the risk of impeding flow, result in less shear stress and total pressure at

the wall of the vessel and reduce the incidence of extravasation. Our clinical observations support this hypothesis as at our institution we observed fewer incidents of contrast extravasation for CTA studies when we changed to a less viscous medium with other parameters unchanged similar to other published work. We postulated that this occurs due to the increased impedance to flow due to the higher contrast viscosity resulting in higher wall shear stress and pressure and we aimed to support this with numerical simulations. Clinically Davenport et al. [7] have established that for higher viscosity media, warming contrast media to body temperature prior to injection and thus reducing media viscosity significantly reduces the incidence of contrast extravasations ($p<0.05$).

2. Methods and Materials

The flow of contrast within an upper limb vein (5 mm diameter, based upon usual distended size of an adult human antecubital vein) is modelled using computational fluid dynamics (CFD) for clinically used size 18G and 20G cannulas, at flow rates ranging from 3 ml/sec to 7 ml/sec for five commonly used non-ionic contrast media of different viscosities but similar osmolalities. Comparisons of total pressures generated and local shear stress profiles are made at flow rates generating equal iodine fluxes. In the CFD modelling we assumed that the blood-flow through the vein model is incompressible with a dynamic viscosity of 3.71×10^{-3} Pa.s and a density of 1060 $kg.m^{-3}$ assigned as constant at a body temperature of 37°C. The governing equations of motion of the flow field are considered as the Navier–Stokes equations, which have been approximated by a low Reynolds number standard k-ω turbulence model with a shear flow correction scheme.

In addition, a mixture multiphase model is applied in order to simulate the injection of contrast through the vein model. The physical properties of the contrast media and the boundary conditions used in the simulation are further described in the following two sections with brief technical details on the CFD techniques and parameters analysed.

2.1. *Geometry and Material Properties*

The configurations for delivering contrast into a patient vein in clinical application are shown in Fig. 1 and serve as the computational models. The two models share the same dimensions e.g. having the same inner diameter of vein (D) and cannula (d) and the length of vein (L) and catheter (s), but the angle (α) measured from the longitudinal axis of the vein is varied. In the computation, we have taken D=5mm, L=100mm, s=32mm, and the intravenous cannula is first inserted at $\alpha=45^{o}$ and its tip rests at the posterior wall of the vessel (Fig. 1a). In the

second model, the catheter is inserted at a shallow angle ($\alpha \approx 5°$) to the vessel with its tip located in the centre of the vessel (Fig. 1b). In order to clarify the effects of the inner diameter of cannula on the flow parameters, the diameter for the 20G cannula is set as d=1mm while for 18G d=1.2mm. Eventually, we have four physical setups for our computational modelling: two from the angular configuration and the other two from the variation of the cannula diameter.

Blood with its constant properties specified in the previous section initially streams into the vein from the vein inlet marked as '1' (Fig. 1) at a mean velocity of 0.10422 $m.s^{-1}$ and exits through the outlet marked as '2'. When the CM is injected into the cannula from the inlet marked as '3', it is expelled through the tip '4' and starts to mix with the blood, and subsequently the CM mixed with the blood is carried through the downstream of the vessel.

Five contrast media were tested and their density, viscosity, osmolality and volume flow rate in the cannula are listed in Table 1. To keep the iodine flux at a specified rate (e.g. 1.5, 1.8, 2.0, 2.2 gI/sec) the flow rate for each specimen is varied accordingly.

2.2. *Numerical Simulations*

The injection process of CM into blood through a vein represents a typical liquid-liquid based two-phase fluid flow [8, 9]. The blood is considered to be a continuous phase while the drug / CM is treated as a dispersed phase with a size of the cannula inner diameter being modelled by the mixture model [9] which solves the equations for the mass continuity and momentum conservation of the CM-blood mixture and for the volume fraction of the CM phase. The Reynolds number based on the flow through the catheter is within the range of 431–1613, depending on the flow rate in the catheter as well as on the density and viscosity of the contrast. It is however eminent that the jet releasing from the catheter will create a strong separation zone inside the vein with a sharpened velocity gradient in the interface between the blood and jet flows. To tackle this issue properly, the low Reynolds number k-ω turbulence model [10] with a shear stress transportation correction is used since the separation would induce large scale turbulence. This standard k-ω turbulence model precisely takes the shearing effect between the high velocity jet flow from the cannula and its surrounding low velocity blood flow. This turbulence model has been successfully applied over the years into various other physiological flow conditions, e.g. see [11-13].

In the numerical simulation, a second order upwind scheme was used to discretise the governing differential equations at a specified discrete mesh volume of total 142,000 cells

(Grid 2). A hexahedral mesh was generated inside the cannula while the mesh inside the vein was a hexahedral / tetrahedral hybrid type. A mesh independence study applying the cell volumes of 108,000 (Grid 1) and 167,000 (Grid 3) was conducted to check the stability of the numerical results as well as their sensitiveness on the mesh choice. The characteristic edge length of the mesh in the cannula and vein for Grid 1 was 0.16 mm and 0.52 mm, respectively; while the characteristic edge length of the mesh wase reduced in Grid 2 (0.13mm, 0.48mm) and Grid 3 (0.13mm, 0.4mm). When the result of the maximum total pressure in an angular configuration was compared between the three grids, we found that the variation was about 11% between Grid 1 and Grid 2. But, the result between Grid 2 and Grid 3 was very close with only about 1.15% variation. The maximum wall stress also compared very well between Grid 2 and Grid 3 and the variation was only about 1.02%. Thus, Grid 2 mesh setup was proved to be sufficient to numerically resolve the flow field in the angular configuration. Likewise, the same mesh (Grid 2) was applied in the centre configuration.

Moreover, a pressure based implicit numerical scheme was chosen along with the SIMPLE pressure-velocity coupling [8], where the pressure at cell surfaces was interpolated with known pressures at nearby nodes.

3. Results

3.1. *Contrast distribution and flow profiles*

Fig. 2(a) shows the unsteady-state concentration/volume fraction distribution of 300 Iopromide (Ultravist) injected at a flux rate of 1.5 (gI/sec) through the 20G intravenous catheter that is placed in the vein at an angle of 45^{o}. Two different time-steps ($dt = 10^{-3}$ and 10^{-4} sec) were initially tested for the unsteady simulations in this selected case and it was found that the results obtained by both were very similar to each other, therefore it was concluded that either of these two *dt* magnitudes were suitable for the unsteady simulations.

Results shown in Fig. 2a were simulated with $dt = 10^{-3}$ sec and presented at a randomly selected time-step, giving the simulation time $t = 2\times10^{-2}$ sec (frame i) to 2 sec (frame xvi), after which the dose distribution flow becomes steady-state. Hence, the rest of the simulation cases were chosen to run under the steady-state condition by ignoring the time-step, which allows us to massively save the computational time for each of the models investigated.

In Fig. 2, the colour contour bar is placed on top to indicate the level of contrast concentration in the vein in the form of magnitude of its volume fraction. Thus the red colour shows the presence of maximum contrast while the blue shows no contrast or in other words

a presence of the maximum level of blood in the vein. The contrast releasing from the tip of the catheter slightly diffuses but mainly travels along and over the vein wall (frames i-v). However, as the catheter tip in this case is directed obliquely to the wall, the fluid friction plays an important role to gradually form a recirculation zone in the vein (frames vi-xv), which eventually becomes stationary at around 2 seconds of the injection time (as shown in the last frame xvi). This recirculation has also a clinical impact since it somewhat creates a blockage inside the vein, causing obstruction to the blood flow through the vein during injection (this issues will be revisited in more detail in the next section when the velocity results and flow pathlines are presented).

Additionally, the placement of the catheter tip at the centre of the vein creates a relatively shorter recirculation zone with the dose concentration higher along the vein centre, as seen in Fig. 2b. Interestingly, the behaviour of the contrast spreading and decaying in magnitude along the vein is typical of a free shear flow of a round jet observed in other engineering contexts.

The velocity profiles calculated for both the catheter orientations have also been compared in Fig. 3. In the case of the catheter placement at 45° near the wall (Fig. 3a) the velocity magnitude increases by about 0.5 $m.s^{-1}$, indicating more dominant effects of the turbulent mixing of the contrast jet released from the tip with the blood flow. Additionally, the obliquely placed tip caused the jet to extend over the vessel wall while for the catheter placed at the centre the jet is more spread around and close to the mid-zone of vessel with the velocity magnitude decreasing as the distance from the tip increased.

In both the cases, the velocity contour further indicates that the free shear layer separating from the tip reattaches to the top vessel wall and causes the recirculation region to form within the vein (also seen in Figs. 2). As a result, the velocity magnitude increases above the tip towards the regime of top vessel wall due to the presence of eddies.

Further evidence to the nature of the flow eddies present within the vein are also given in Fig. 3 where the flow pathlines obtained from the two injection setups are presented. Note that the colour in the pathlines represents the concentration of contrast as already seen in Fig. 2. The most interesting point is in the structure of eddies forming from the catheter tip. The centrally placed catheter creates eddies in a more rounded shape and these are seen to remain coherent for a distance downstream of the catheter in contrast to the case of the other catheter placement. Moreover, the eddy strength as well as its length is found to be much shorter in

the centre case, but the similarity is seen in the far downstream of the vein where the mixture of contrast with blood flows smoothly and exits the domain. Qualitatively, the flow profiles and the behaviour of contrast mixing were found to be similar at the other iodine flux rates.

3.2. *Assessment of the Vein Wall Shear Stress and Pressure*

Qualitative and quantitative differences in the distribution of shear stresses and total pressure on the vein wall for the different contrast media injected at a constant iodine flux rate of 1.5 gI/sec in the 20G catheter placed at 45^{o} are shown in Figs. 4 and 5 respectively. The injection region has been zoomed in to clearly visualise the effects on the wall, and the contour levels are generated using their extremum for the purpose of quantitative comparison and assessment. Generally, the results for all the contrast media depict that there is a core region of forming the shear stress and pressure on the vessel wall due to the jet impingement of injection contrast inside the vein. However, the magnitude is affected by both the material properties and injection volume flow rate of the contrast. Most notably, the wall shear stress for 300 Iopromide (Ultravist) (Fig. 4b) is significantly and consistently lower than for 300 Iohexol (Omnipaque) (Fig. 4a) despite the same injection rate (5 ml/sec). The low contrast viscosity and other parameters (listed in Table 1) plays a significant role here and appears to lower the shear stresses for 300 Iopromide. There is a systematic drop in the vessel wall pressure from frame (a) to (e) in Fig. 5 due to the lowering of the flow rate and their maximum magnitude will be compared in the next section.

For the Iodine fluxes ranging 1.5 gI/s–2.2 gI/s the least viscous contrast media generated the least maximum wall shear stress in all the simulations. Total wall pressure is proportionally affected by the flow rates (Figs. 6 and 7), however, the wall shear stress appears mostly affected by the media viscosity. In addition, the flow rate appears to be a less important factor in the latter, with the higher flow rates of the less viscous media generating less shear stress than the lower flow rates of more viscous media (Figs. 8 and 9). Comparison of the wall stress for the iodine flux 1.8 and 2.0 gI/sec for 300 Iohexol and 300 Iopromide indicate that a higher flow rate of the more viscous Iohexol for flux 1.8 gI/sec generates more wall shear stress than the less viscous Iopromide does, even when the latter flows at a faster rate with generation of higher iodine flux (2.0 gI/sec).

The characteristics of the maximum wall shear stress and the total pressure of the 18G cannula are similar to those for the 20G cannula shown above. The detailed charts of the 18G cannula can be found in the electronic supplementary file.

4. Discussion

Flow rates of contrast are frequently pre-determined by the local institutional CT protocols for each examination with reduction in flow rates being allowed to accommodate suboptimal venous access, smaller intravenous catheters and patient specific factors. This process is predominantly within the remit of the duties of the operator who assigns a flow rate of contrast based on observational data and triggered pressure alarms generated by the contrast-injecting pump. Other than iodine content (e.g. 300 versus 400 'strength') the type of contrast medium used in terms of chemical formulation is often not deemed an important factor clinically in determining the flow rate provided that the final outcome of a diagnostic scan is achieved. This certainly applies to scans of the abdomen in the portal venous phase where diagnostic scans can be achieved with lower flow rates than required for CTA as it is the total iodine 'dose' that is important in obtaining opacification of the solid abdominal organs at a set delay time. However for CT angiography, cardiac/coronary or otherwise, a diagnostic scan requires a high iodine flux and consequently higher rates of flow with more iodine rich media.

For media exhibiting similar characteristics, viscosity appears to be the determining factor in causing higher vessel wall shear stress as in the case of 300 Iohexol compared with 300 Iopromide. The latter is less viscous and despite similar osmolality, the same flow rates, iodine flux and total pressure generated, the less viscous media generates less wall shear stress at all the simulated rates of injection. This held true in all the simulations performed with the effect being highest when the angle of the intravenous catheter was at 45^{o} to the vessel wall. Indicative graphical representations of results are depicted from different simulation scenarios, however, all exhibiting a constant trend.

In addition, the total pressure is composed of the fluid static and dynamic pressures. The static pressure induces additional stresses to the vein wall and the base cuff pressure (P) of a forearm vein is measured to be 50 mmHg [14]. Considering the vein inner radius (r) of 2.5 mm with a uniform wall thickness (h) of 0.54 mm [15], the base circumferential stress in the vein wall (S_θ) can be estimated by using the Laplace law, $S_\theta = P\left(\frac{r}{h} - \frac{1}{2}\right)$ [16, 17]. Where, the last term in the right hand side of the formula contributes to the radial stress and may be neglected for a thin-wall membrane tube only when the critical value of r/h is equal or over 20 as reported in [18]. However, the ratio in our model is 4.63, suggesting a thick-wall vein structure, thus the last term in the right-hand side has to be retained to avoid any over-

prediction in the wall stress. Moreover, if *P* is an incremental fluid static pressure above the baseline pressure in a vessel wall, the stress magnitude derived (S_θ) will be the corresponding incremental circumferential stress, ΔS_θ. The incremental fluid static pressure is shown in Table 2 for the 45° 18G angular cases. The estimated incremental circumferential stress in the vein wall under each static pressure is also presented in the table. It is shown that the maximum incremental stress (ΔS_θ) can be as high as 22.16 kPa, which is moderately comparable with the base value (S_θ) of 27.17 kPa. The peak incremental stress usually increases the vein wall stress level and thus could make a patient uncomfortable with pain during and after the contrast injection. In the cases where the catheter is placed at the centre of the vein, the incremental circumferential stress is found to be within the range of 1.30 kPa – 3.85 kPa, which is much lower than that shown in the 45° angular cases, thus suggesting that placing the catheter tip further off the wall is helpful in reducing the stress level caused by the injection.

However, the influence of the dynamic pressure on the stress level in the vein wall is a localised phenomenon since it only induces additional stress in the local area where the ejecting jet impinges. This effect is so complex that a 3-D fluid-structure interaction study should be performed and obviously, this was out of the scope of this paper. However, this can still be explained qualitatively by making use of the momentum theory in fluid mechanics. Assuming the ejecting jet released from the catheter tip attacks the vein wall at an angle that is equal to the inclination angle α and with a velocity V_j. Then the jet is reflected back to the blood main stream with the same angle and velocity. By using the momentum theory [19] the normal force applied by the jet on the vein wall is estimated from $F = 2\rho_j V_j^2 \sin\alpha = 2\rho_j \left(\frac{4Q_j}{\pi d^2}\right)^2 \sin\alpha$, where ρ_j is the contrast density, Q_j is the volume flow rate and *d* is the catheter inner diameter. Injecting contrast through a narrow diameter catheter at a higher inclination angle and flow rate as well as density results in an increased dynamic force and thus subsequently raises the local vein stress level. However, when the catheter tip is moved to the centre of the vein, the inclination angle is reduced and eventually, the normal force is lowered and subsequently has a lower risk of potential tissue damage and contrast extravasation.

Furthermore, the wall shear stress (WSS) of blood flow in human healthy veins usually varies from 0.3 Pa to 0.78 Pa [20, 21]. In our simulation, the average WSS on the vein model

without placing a catheter inside by using a laminar flow model is predicted to be 0.62 Pa, which appears to be consistent. In the cases of the catheter placed in the centre of the vessel, the maximum WSS on the vessel wall is found to be in the range 46.9 Pa – 107.4 Pa, while it is 293 Pa – 775.3 Pa in the cases of the catheter inserted at 45° and resting at the posterior wall of the vessel. A quantitative assessment of the numerically predicted WSS magnitude in relation to the contrast extravasation though is not possible to make due to the absence of appropriate data, other published research on the hemodynamic roles of WSS in vessels, for example [22], suggests that the higher magnitude of WSS might have consequences in potentially damaging endothelial cells in the vein wall or causing permanent injury in its soft tissue. In the poorest case, the highest WSS may also trigger the incidence of contrast extravasation and thus placing the catheter tip to the centre of the vein might be a better option. Furthermore, the risk factors of intravenous (IV) contrast medium extravasation are also associated with injection technique and patient circumstance as discussed in [23]. The former includes the type of catheter used, puncture in vein, duration of injection, as well as use of any automatic injector. The patient circumstance, on the other hand, usually includes the size of vein used, fragile and damaged vein, peripheral vascular diseases, and weakened or impaired ability. It was argued in [24] that the vein spasm, pre-existing vein phlebitis, and small veins may also be ruptured by the force of a high pressure injection.

Further to the aforementioned conclusions drawn from the data, it is also interesting to note that the scales on the graphical representations are significantly different with intravenous cannula size and angle within the vessel also contributing greatly to the overall wall pressure and vessel wall shear stress. Although these findings are expected, the magnitude of their significance numerically is noteworthy. Optimum placement of a catheter tip in the centre of a vessel dramatically reduces the total wall pressure ($1/30^{th}$) and the wall shear stress ($1/4^{th}$) although in real world situations this may not be easily controlled. This also indicates that placing a catheter tip near a vein branch point where it is more likely to be directed against a wall is less ideal. Additionally, the use of a larger calibre catheter (18G in comparison to 20G), according to the numerical data, reduces the wall pressure by ~20% whilst it almost halves the values for the wall shear stress.

There are several limitations to our current study. Firstly, we have studied a ‘vein’ with a fixed diameter and no distensibility without branch points, but in reality veins are distensible and this will have an influence – potentially increasing the importance of wall shear stress as a parameter. Secondly, we do not know for certain which component of the total pressure is

most important in the pathophysiology of vein rupture and although we suspect empirically and from studies in arterial plaque and aneurysm ruptures that the wall shear stress is important, further study of this is required. Thirdly, the temperature of the administered CM has been kept constant at 37°C which is the theoretical ideal. In the real world situation, however, the temperature of the CM will often be between room and body temperature. As the temperature of the CM strongly influences the contrast viscosity, there may be further significant differences here which we also intend to model in future work. Furthermore, although a representative selection of CM has been assessed, not all commercially available CM have been evaluated. Lastly, we have not modelled cannulae other than standard types with a single end hole, other designs may well produce significant differences and are also worthy of future study in this respect. In addition, suitable experimental techniques are proposed for verifying the numerically predicted results.

5. Conclusion

The type of contrast media and in particular its viscosity may significantly influence the probability of extravasation, particularly for CT angiography, especially with less than ideally placed smaller intravenous cannulae. The computational results support our original hypothesis relating the viscosity of contrast media to extravasation potential and in addition have emphasised and numerically quantified other parameters potentially within our control (specifically cannula size) relating to intravenous cannulation that should be better managed if extravasation risk is to be minimised.

The multiphase mixture model chosen in the CFD simulations takes the effects of blood mixing with contrast medium by assuming the mixture density and viscosity being a linear combination of those of the two media determined from their volume fraction. Flow of the two fluids is considered to be continuous and immiscible, and their interactions are modelled with the drag force applied on a spherical droplet of contrast medium with two-phase slip velocity and a constant diameter that is equal to the inner diameter of the catheter. In spite of the simplicity in the mixture model used, the present findings on the contrast injection flow physics and patterns show consistency with other studies focused on the saline injection in blood vessel [25, 26]. Moreover, Ghata et al. [25] reported that the maximum WSS and

pressure on blood vessel were caused by the saline injection, a finding that also strongly corroborates with our results. These studies used the same mixture model.

Acknowledgement

The authors are grateful to Bayer Healthcare Ltd. for providing financial support in order to complete the research simulations. The funder had no role in study design, data collection and analysis, decision to publish, or preparation of the manuscript.

Conflict of interest

The authors declare that they do not have any conflict of interest with the funder and any other party relating to employment, consultancy, patents, products in development, marketed products, etc.

Ethical approval

Not required.

References

1. Singh J, Aditya Daftary A, Iodinated Contrast Media and Their Adverse Reactions, J Nucl Med Technol 2008; 36:69–74.
2. Persson B P, Hansell P, Liss P, Pathophysiology of contrast medium–induced nephropathy, Kidney Int., 2005; 68:14–22.
3. Thomsen H S, Morcos S K: Contrast media and the kidney: European Society of Urogenital Radiology (ESUR) guidelines. Br J Radiol; 2003; 76:513–518.
4. Wang C L, Cohan R H, Ellis JH, Adusumilli S, Dunnick NR. Frequency, management, and outcome of extravasation of nonionic iodinated contrast medium in 69,657 intravenous injections. Radiology. 2007; 243:80–87.
5. Federle MP, Chang P J, Confer S, Ozgun B. Frequency and effects of extravasation of ionic and nonionic CT contrast media during rapid bolus injection. Radiology. 1998; 206:637–640.
6. Selek H, Ozer H, Aygencel G, Turanli S. Compartment syndrome in the hand due to extravasation of contrast material. Arch Orthop Trauma Surg. 2007; 127:425-427

7. Davenport M S, Wang C L, Bashir M R, Neville A M, Paulson E K, Rate of contrast material extravasations and allergic-like reactions: effect of extrinsic warming of low-osmolality iodinated CT contrast material to 37°C. Radiology. 2012; 262: 475-484.
8. FLUENT 6.3. Tutorials Guide. USA: Fluent Inc; 2007.
9. Rhode S, Paul M C, Martens E, Campbell D F. Simulation of haemodynamic flow in head and neck cancer chemotherapy. BioMed Eng OnLine. 2011; 10(104): 1-11.
10. Wilcox D C. Turbulence modelling for CFD. La Canada California: DWC Industries; 1993.
11. Ryval J, Straatman A G and Steinman D A. Two-equation turbulence modelling of pulsatile flow in a stenosed tube. ASME J of Biomechanical Engineering. 2004; 126: 625-635.
12. Paul M C, Larman A. Investigation of spiral blood flow in a model of arterial stenosis. Medical Engineering Phys. 2009; 31:1195-1203.
13. Linge F, Hye M A, Paul M C. Pulsatile spiral blood flow through arterial stenosis. Computer Methods in Biomechanics and Biomedical Engineering. 2014; 17: 1727-1737.
14. Thalhammer C, Aschwanden M, Odermatt A, Baumann U A, Imfeld S, Bilecen D, Marsch S C and Jaeger K A. Noninvasive central venous pressure measurement by controlled compression sonography at the forearm. J Am Coll Cardiol. 2007; 50(16): 1584-1589.
15. Travers J P, Brookes C E, Evans J, Baker D M, Kent C, Makin G S and Mayhew T M. Assessment of wall structure and composition of varicose veins with reference to collagen, elastin and smooth muscle content. Eur J Vasc Endovasc Surg. 1996; 11: 230-237.
16. Wesly R L R, Vaishnav R N, Fuchs J C A, Patel D J and Greenfield J C. Static linear and nonlinear elastic properties of normal and arterialized venous tissue in dog and man. Circulation Research. 1975; 37: 509-520.
17. Vaishanv R N, Young J T, Janicki J S and Patel D J. Nonlinear anisotropic elastic properties of the canine aorta. Biophysical Journal. 1972; 12: 1008-1027.
18. Ventsel E and Krauthammer T. Thin Plates and Shells, New York: Marcel Dekker, Inc., 2001.
19. Streeter V L, Fluid Mechanics (third edition), New York: McGraw-Hill Book Company, Inc., 1962.

20. Wiewiora M, Piecucha J, Gluck M, Slowinska-Lozynsk L and Sosada K. Shear stress and flow dynamics of the femoral vein among obese patients who qualify for bariatric surgery. Clinical Hemorheology and Microcirculation. 2013; 54: 313–323.
21. Misra S, Woodrum D A, Homburger J, Elkouri S, Mandrekar J N, Barocas V, Glockner J F, Rajan D K and Mukhopadhyay D. Assessment of wall shear stress changes in arteries and veins of arteriovenous polytetrafluoroethylene grafts using magnetic resonance imaging. Cardiovasc Intervent Radiol. 2006; 29: 624–629.
22. Malek A M, Alper S L and Izumo S. Hemodynamic shear stress and its role in atherosclerosis. JAMA. 1999; 282(21): 2035–2042.
23. Pacheco Compana F J, Gago Vidal B and Mendez Diaz C. Extravasation of contrast media at the puncture site: strategies for management. Radiologia. 2014; 56:295-302.
24. Cohan R H, Ellis J H, Garner W L. Extravasation of radiographic contrast material: Recognition, prevention, and treatment. Radiology. 1996; 200: 593–604.
25. Ghata N, Aldredge R C, Bec J, Marcu L. Computational analysis of the effectiveness of blood flushing with saline injection from an intravascular diagnostic catheter. Int J Numer Method Biomed Eng. 2014; 30(11): 1278–1293.
26. Choi HW, Jansen B, Birrer D. Kassab GS effect of saline injection mixing on accuracy of conductance lumen sizing of peripheral vessels. PLoS ONE. 2013; 8(9): e74622.

Iodine Flux (gI/sec)	**1.5**	**1.8**	**2.0**	**2.2**	**Osmolality (osm/kg)**	**Viscosity (Pa.s)×10^{-3}**	**Density (kg/m^3)**
	Flow rate (ml/sec)						
300 Iohexol (Omnipaque)	5.0	6.0	6.7	7.3	0.64	6.3	1422
300 Iopromide (Ultravist)	5.0	6.0	6.7	7.3	0.59	4.7	1332
350 Iohexol (Omnipaque)	4.3	5.1	5.7	6.2	0.78	10.4	1480
370 Iopromide (Ultravist)	4.1	4.9	5.4	5.9	0.77	10.0	1399
400 Iomeprol (Iomeron)	3.8	4.5	5.0	5.5	0.72	12.6	1460

Table 1: Contrast media flow rates compared for given iodine flux and their physical characteristics.

Iodine Flux (gI/sec)		**1.5**	**1.8**	**2.0**	**2.2**
300 Iohexol (Omnipaque)	Flow rate (ml/sec)	5.0	6.0	6.7	7.3
	ΔP (kPa)	2285	3796	4548	5367
	ΔS_θ (kPa)	9.43	15.68	18.78	22.16
300 Iopromide (Ultravist)	Flow rate (ml/sec)	5.0	6.0	6.7	7.3
	ΔP (kPa)	2129	1805	3992	4718
	ΔS_θ (kPa)	8.79	7.45	16.48	18.48
350 Iohexol (Omnipaque)	Flow rate (ml/sec)	4.3	5.1	5.7	6.2
	ΔP (kPa)	2478	3088	3474	4013
	ΔS_θ (kPa)	10.23	12.75	14.34	16.57
370 Iopromide (Ultravist)	Flow rate (ml/sec)	4.1	4.9	5.4	5.9
	ΔP (kPa)	2554	2698	2974	3611
	ΔS_θ (kPa)	10.54	11.14	12.29	14.91
400 Iomeprol (Iomeron)	Flow rate (ml/sec)	3.8	4.5	5.0	5.5
	ΔP (kPa)	2493	3303	4780	5429
	ΔS_θ (kPa)	10.29	13.64	19.74	22.42

Table 2: Incremental static pressure and circumferential stress in the 45° 18G angular cases.

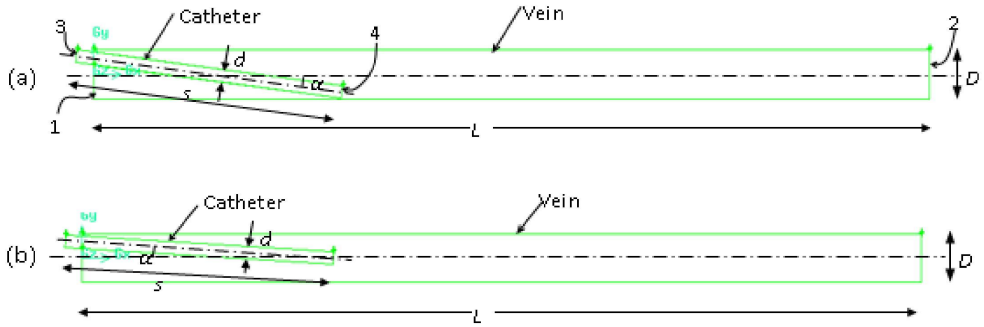

Fig. 1: Two configurations for the catheter placement inside the vein model: (a) 45° angle resting at the posterior of the vein wall, (b) a shallow angle and the tip of the catheter placed in the centre of the vein.

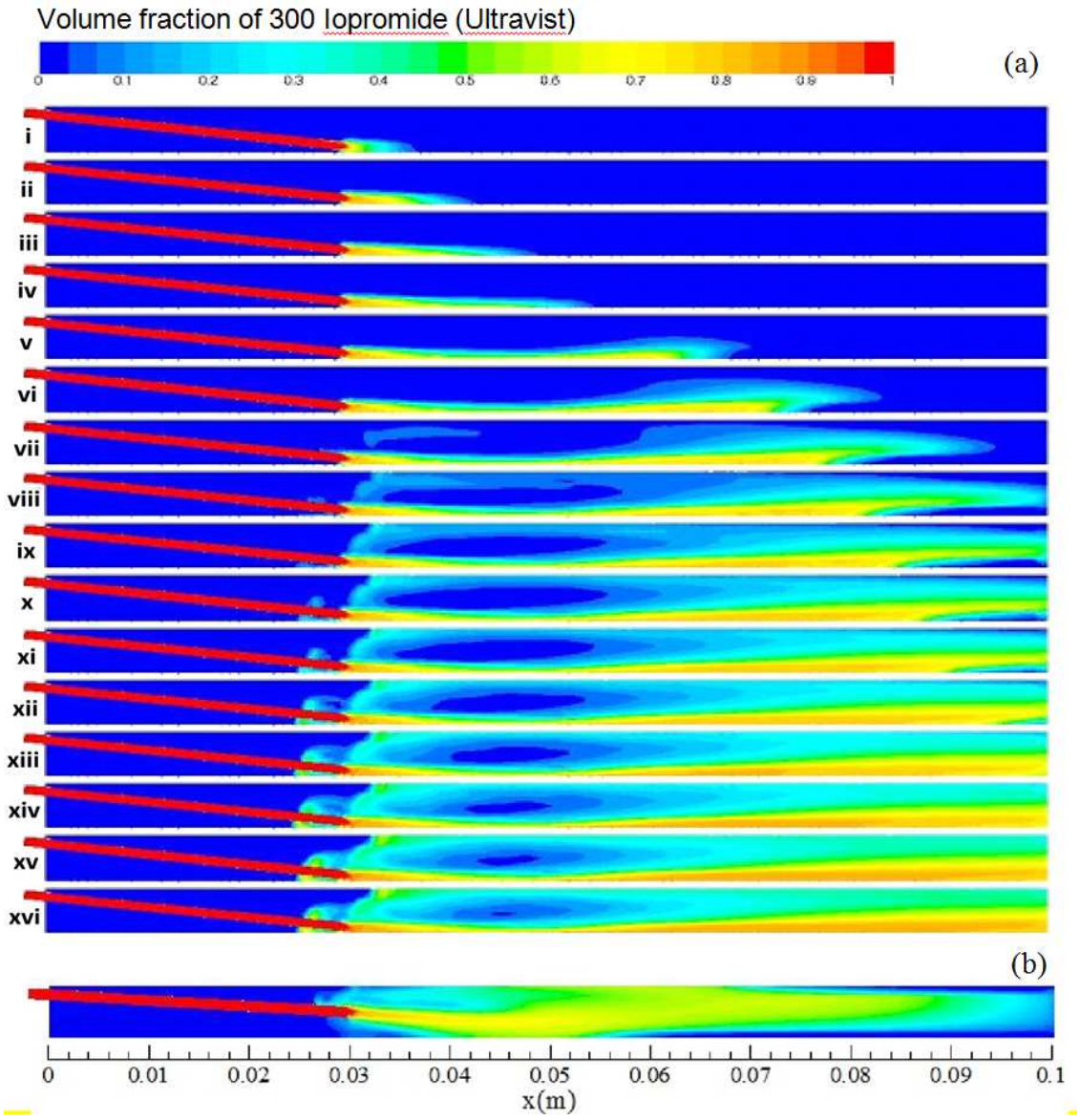

Fig. 2: Unsteady distribution of 300 Iopromide (Ultravist) injected at a flux rate of 1.5 gI/sec through the 20G intravenous catheter placed in the vein at an angle of 45^{o} (a), and concentration of 300 Iopromide (Ultravist) injected through the 20G intravenous catheter placed in the vein centre at the same flux rate.

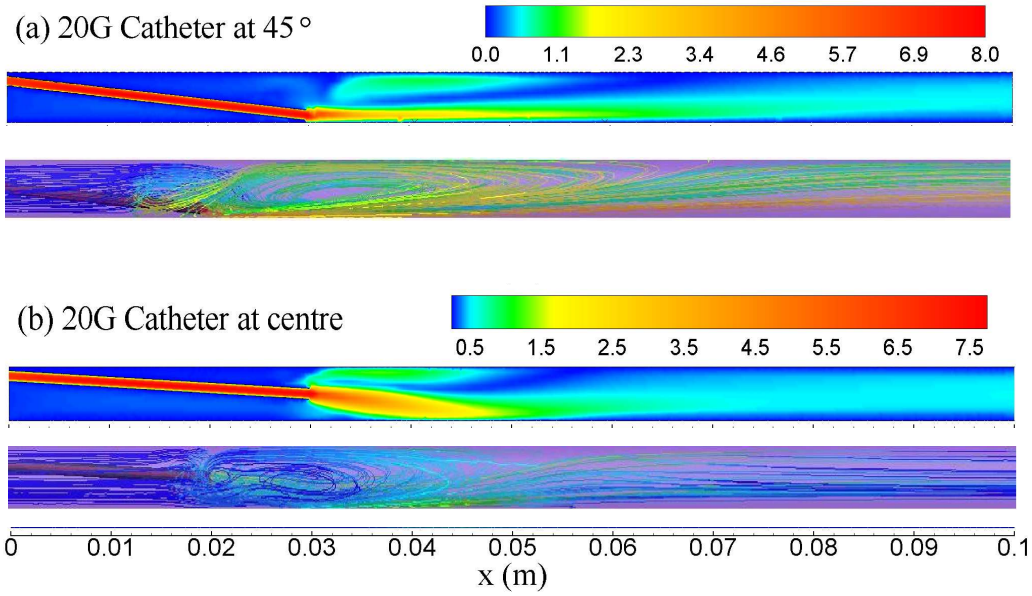

Fig. 3: Comparison of the velocity magnitude and flow pathlines at two different angular orientations for the 20G catheter, the pathlines coloured by the dose concentration

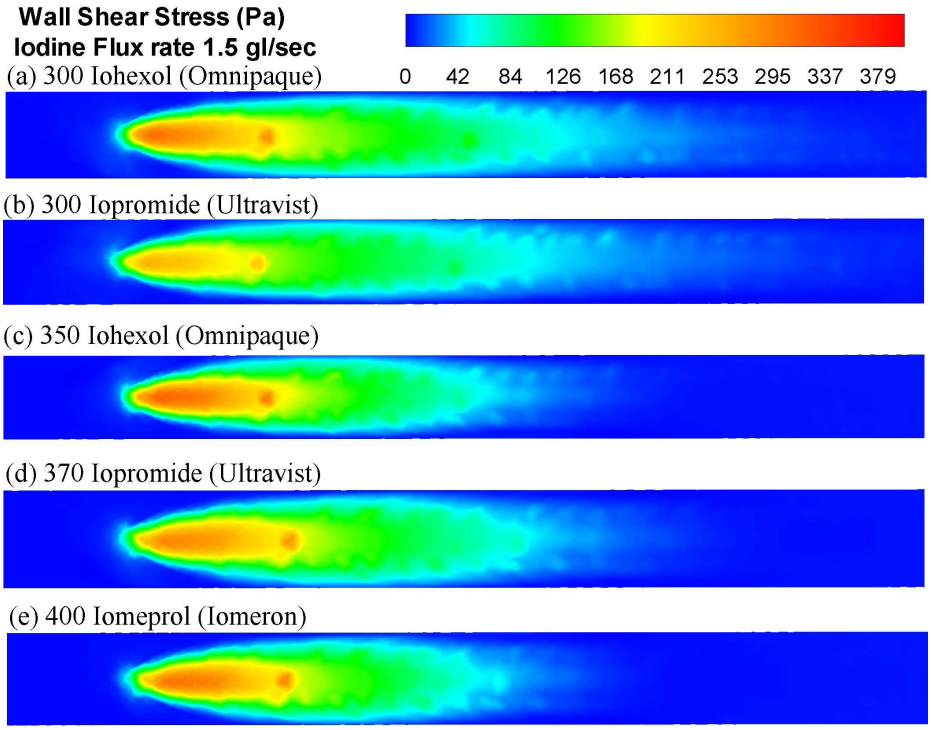

Fig. 4: Comparison of the vessel wall shear stress for different contrast media at an iodine flux rate of 1.5 gI/sec for the 20G catheter placed at 45^{o}.

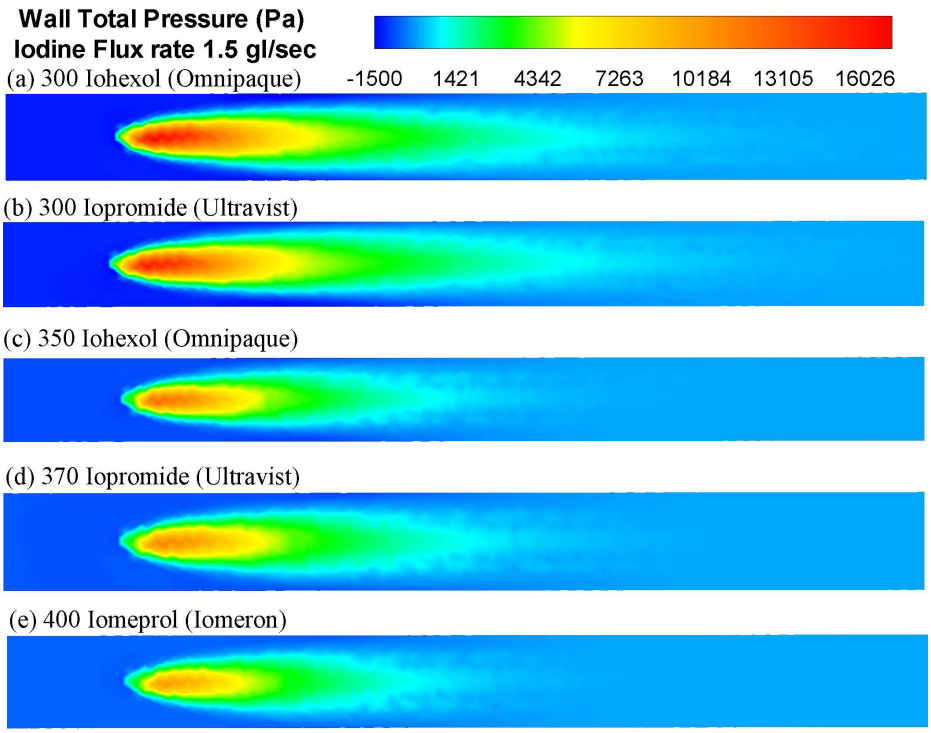

Fig. 5: Comparison of the vessel wall total pressure (133.32 Pa = 1 mmHg) for different contrast media at an iodine flux rate of 1.5 gI/sec for the 20G catheter placed at 45^{o}.

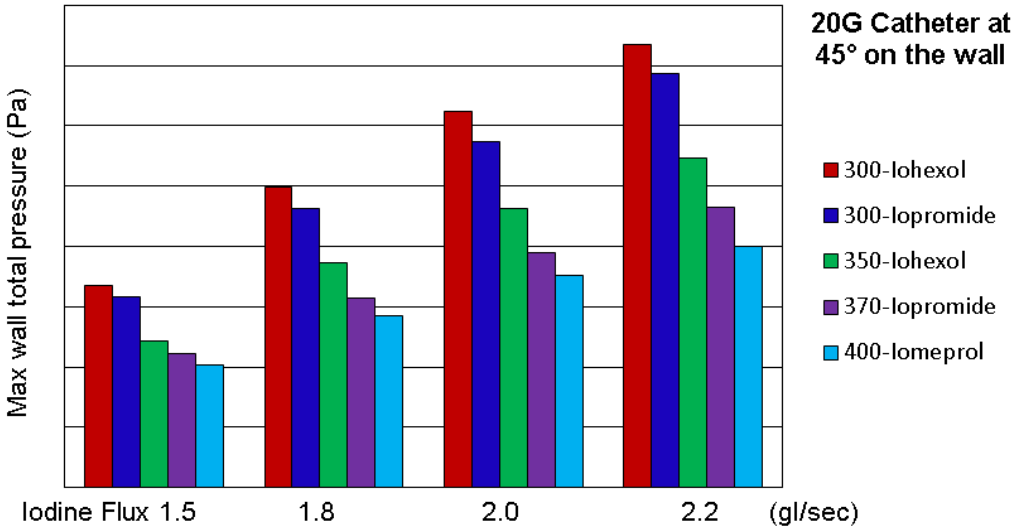

Fig. 6: Maximum wall total pressure for all the contrast media and iodine fluxes in the 20G IV catheter at 45^{o}.

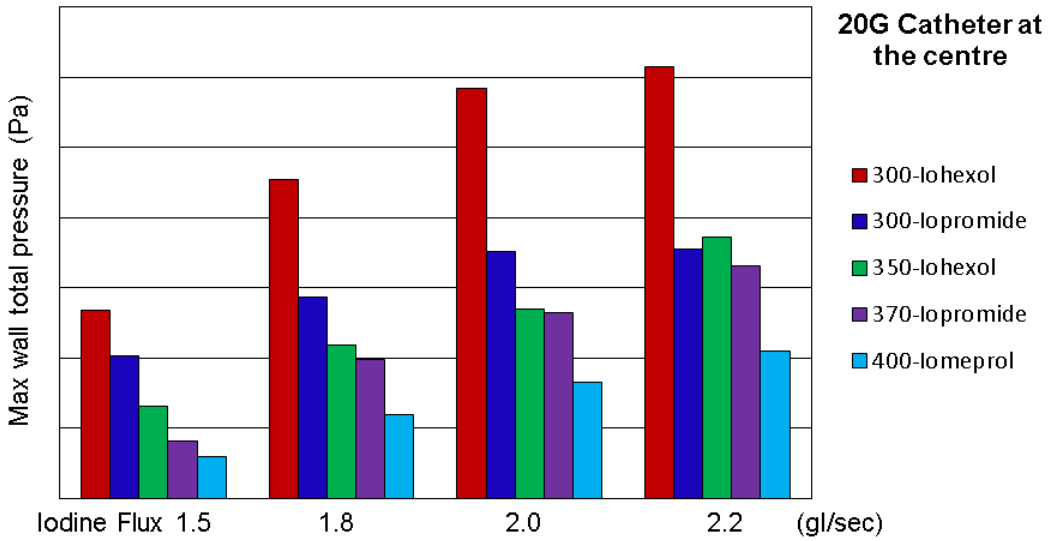

Fig. 7: Maximum vessel wall total pressure for all the contrast media and iodine fluxes in the

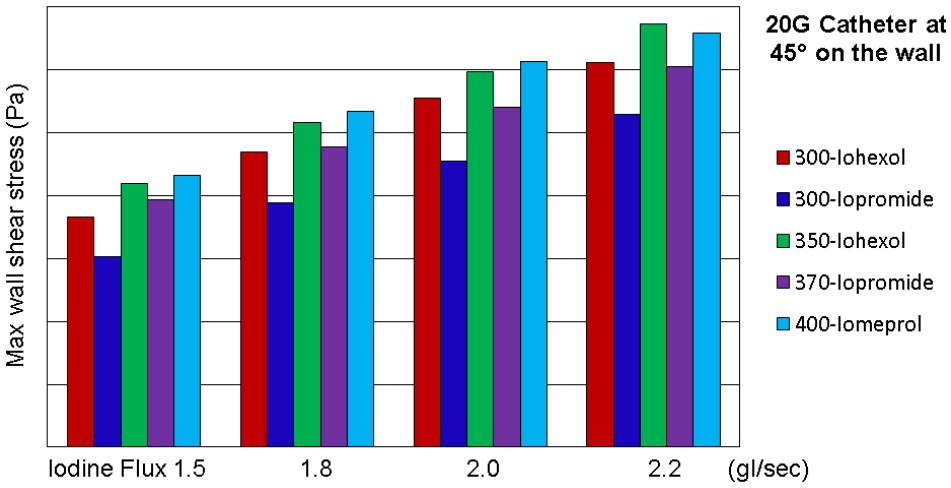

Fig. 8: Maximum vessel wall shear stress for all the contrast media and iodine fluxes in the 20G IV catheter at 45^{o}.

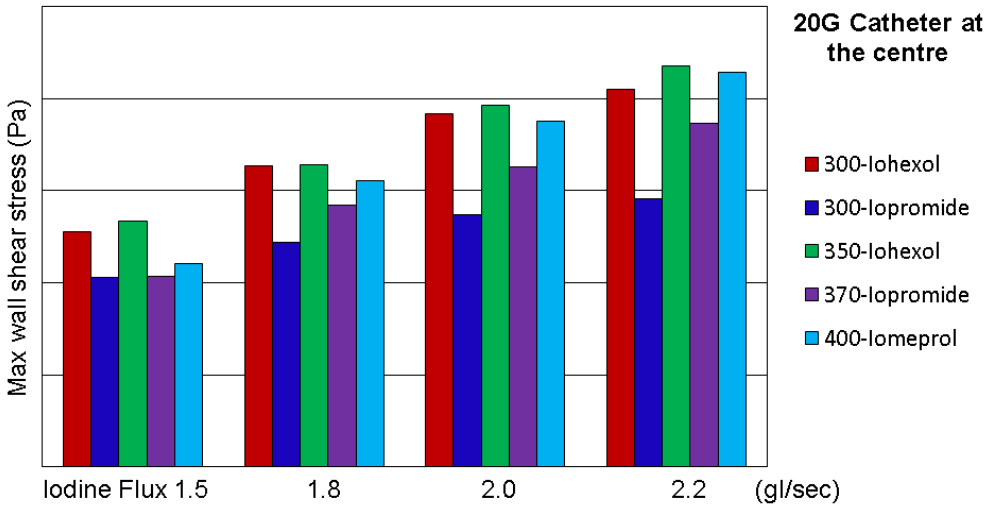

Fig. 9: Maximum vessel wall shear stress for all the contrast media and iodine fluxes in the 20G IV catheter placed at the centre of the vessel.